Geometry Optimization of Organometallic Compounds Using a Modified Extended-Hückel Formalism

François Savary and Jacques Weber*

Department of Physical Chemistry, University of Geneva, 30 quai Ernest-Ansermet, CH-1211 Geneva 4, Switzerland

Gion Calzaferri

Institute for Inorganic and Physical Chemistry, University of Bern, Freiestrasse 3, CH-3000 Bern 9, Switzerland

Received: December 2, 1992

The modified extended-Hückel method suggested recently by Calzaferri and co-workers has been parametrized for organometallic compounds in order to have at hand a semiempirical tool allowing for rapid optimization of their geometries. The model is based on (i) the introduction of an approximate two-body repulsive electrostatic energy term and (ii) the use of a distance-dependent Wolfsberg–Helmholz formula, $K = 1 + \kappa e^{-\delta(R_{AH}-d_0)}$, for 1–2 and 1–3 interactions. The optimum values for the κ, δ parameters determined for given classes of metal–ligand interactions have been found to be transposable to systems exhibiting several types of ligands such as aromatic rings, carbonyls, phosphines, etc. The overall performance of the model is satisfactory, as it leads for a series of more than 30 organometallic compounds to average error bars of 0.058 and 0.039 Å on metal–ring and metal–carbonyl bond distances, respectively, and of 2.6° on bond angles.

I. Introduction

Molecular modeling has recently evolved from the stage of an esoteric tool reserved to computational chemists into a mature field enabling practically every experimentalist to perform his own applications. Indeed, several user-friendly packages can be used today to study, at different levels of sophistication, molecular structure, function, and interaction.[1] However, whereas such investigations can be performed on a routine basis for organic compounds, the situation is different for transition metal complexes, such as organometallics, due to the well-known difficulties associated with an adequate ab initio quantum chemical description of the structure and properties of these compounds.[2-5]

Density functional methods represent undoubtedly in this field a very interesting alternative to the traditional ab initio approach, specially from the point of view of the quality of the results,[6-8] but a full geometry optimization of organometallics using these formalisms cannot yet be qualified as a routine task.

Empirical force field methods, which are powerful tools for building the structure of organics,[9] cannot be easily generalized for d-electron compounds, although some recent results in this area are promising.[10-14] There is therefore still a need for simple computational models, based, for example, on semiempirical quantum chemical methodologies, allowing for rapid and efficient optimization of the geometry of organometallic compounds. Interesting solutions in this direction have recently been suggested: Zerner et al. have parametrized the so-called ZINDO model for organometallic species leading to satisfactory results for the geometries of various complexes;[15] Blyholder et al. have derived MINDO/3 parameters for iron, which allowed them to rationalize the structure of several iron complexes;[16] finally, Li and Jug have developed an extended version of the SINDO1 method to optimize the geometry of transition metal compounds with an accuracy comparable to that of 3-21G ab initio SCF calculations.[17]

On the other hand, the extended-Hückel method (EHMO)[18] in its improved ASED (atom superposition and electron delocalization) form has been shown to describe reasonably well the structural properties of organometallic compounds.[19-21] Recently, Calzaferri et al.[22] and Tupper et al.[23] have discussed and improved

this approach, which led to better structural predictions for small molecules. These authors, however, do not report any parameter development for organometallics.

We therefore present results obtained for the geometry optimization of such compounds using an adequately parametrized EHMO-ASED procedure. This model has been chosen so as to be coherent with our reaction potential method calculating a reactivity index for electrophilic or nucleophilic attack on organometallic compounds and based on extended-Hückel wave functions.[24-27]

II. ASED Formalism

The EHMO model is the simplest quantum chemical method considering all the valence electrons of a system. It is well known that the EHMO model in its original form is, in principle, not able to optimize geometries correctly as it lacks repulsive electrostatic interactions. Anderson and Hoffmann[19] have shown that by introducing a two-body electrostatic correction term, this deficiency can be overcome. The total energy is calculated as[22]

$$E_{tot} = \Delta E_{EHMO} + E_{Rep} \tag{1}$$

where ΔE_{EHMO} is the extended-Hückel binding energy calculated as

$$\Delta E_{EHMO} = E_{EHMO} - \sum_{\mu} b_{\mu}^0 E_{\mu}^0 \tag{2}$$

E_{EHMO} is the "classical" extended-Hückel total energy; b_{μ}^0 and E_{μ}^0 are occupation number and valence-state ionization energy (VSIE) of atomic orbital μ, respectively, the summation over μ running on all the atomic orbitals of the complex. The repulsive energy E_{Rep} is expressed as

$$E_{Rep} = \sum_{A} \sum_{B < A} E_{AB} \tag{3}$$

with E_{AB} originally calculated by Anderson and Hoffmann[19] as

$$E_{AB} = \frac{Z_A Z_B}{R_{AB}} - Z_A \int \frac{\rho_B(\vec{r})}{|\vec{R}_A - \vec{r}|} d\vec{r} \tag{4}$$

where E_{AB} is the repulsive electrostatic energy for the interaction

of atoms A and B, separated by distance R_{AB}, with Z_A, $\bar{R}_A$ and ρ_A being the nuclear charge, position, and electron density of the atom A, respectively, B being more electronegative than A.

Calzaferri et al. have suggested reformulating E_{AB} as follows:[22]

$$E_{AB} = \frac{Z_A Z_B}{R_{AB}} - \frac{1}{2}\left[Z_A \int \frac{\rho_B(\vec{r})}{|\vec{R}_A - \vec{r}|} d\vec{r} + Z_B \int \frac{\rho_A(\vec{r})}{|\vec{R}_B - \vec{r}|} d\vec{r} \right] \quad (5)$$

where the second right-hand term of eq 5 is the arithmetic mean of A–B and B–A attractive interaction energies.

On the other hand, Anderson has suggested improving the model by modifying the off-diagonal EHMO matrix elements in the following way:[20]

$$H_{\mu\nu} = \frac{1}{2}K(H_{\mu\mu} + H_{\nu\nu})S_{\mu\nu}e^{-\delta R}{}_{AB} \quad (6)$$

where $K = 2.25$, δ is an adjustable parameter, whose optimal value is 0.13 Å^{-1}, and R_{AB} is the distance between the atoms bearing the orbitals μ and ν, respectively.

The deficiencies of this approach have been discussed and eliminated by including a distance-dependent exponential factor into the K constant as follows:[22]

$$K_{AB} = 1 + \kappa e^{-\delta(R_{AB}-d_0)} \quad (7)$$

where K_{AB} is the EHMO K parameter used in the nondiagonal Hamiltonian matrix elements $H_{\mu\nu}$, with orbitals μ and ν belonging to atoms A and B, respectively; κ and δ are positive empirical parameters such as $0.75 \leq \kappa \leq 1.25$ and 0.13 Å$^{-1} \leq \delta \leq 0.35$ Å^{-1}, with d_0 being equal to the sum of atomic orbital radii $r_n(A) + r_n(B)$ which are defined by

$$r_n = \frac{1}{\int_0^\infty \frac{1}{r} R_{nl}^2(r) r^2 \, dr} \quad (8)$$

For single-ζ Slater-type orbitals, one has

$$r_n = \left(\frac{n}{\zeta}\right) a_0 \quad (9a)$$

whereas for double-ζ Slater-type orbitals, with exponents ζ_1, ζ_2 and coefficients c_1, c_2

$$r_n = \frac{n}{c_1^2 \zeta_1 + c_2^2 \zeta_2 + \frac{2^{2n}(\zeta_1\zeta_2)^{n+1/2}}{(\zeta_1 + \zeta_2)^{2n}}} \quad (9b)$$

where a_0 is the Bohr radius.

This reformulation of the EHMO method leads to a significant improvement of the potential energy curves of diatomic and small organic molecules, especially after optimization of the κ, δ parameters for given classes of compounds.[22] An investigation on the geometry of organic molecules containing C, H, O, N, and S has led to the result that bond lengths and bond angles can well be described with $0.85 < \kappa < 1.215$ and $\delta = 0.35$ Å^{-1}. As an example the error on the calculated bond lengths is on the order of 1% only if $\kappa(C,sp) = 0.85$, $\kappa(C,sp^2) = 0.975$, $\kappa(C,sp^3) = 1.215$, and $\delta = 0.35$ Å^{-1} is applied.[28] Our purpose here is to extend this parametrization to organometallic compounds.

As a first step, we have decided to simplify the calculation of d_0 by approximating it as the sum of the covalent radii R_{covA} and R_{covB} (taken from ref 29), which transforms eq 7 as

$$K_{AB} = 1 + \kappa e^{-\delta[R_{AB}-(R_{covA}+R_{covB})]} \quad (10)$$

In a second step, geometry optimizations have been carried out for given classes of organometallics by modifying the constants κ and δ of eq 10, and it has been found that the calculated structural properties were relatively sensible on the basis of the values of these parameters. It seemed thus possible to optimize these

TABLE I: Values of κ, δ Parameters for Classes of Atomic A–B Interactions[a]

atom A	atom B	κ	δ Å^{-1}
	1–2 Interactions		
metal	carbon (cyclobutadienyl)	0.40	0.35
metal	carbon (cyclopentadienyl)	0.50	0.40
metal	carbon (benzene)	0.40	0.50
metal	carbon (naphthalene)	0.50	0.60
metal	carbon (carbonyl)	0.10	1.90
metal	phosphorus	0.20	2.00
carbon (carbonyl)	oxygen (carbonyl)	1.20	0.00
carbon	hydrogen	0.60	0.90
carbon	phosphorus	1.20	0.00
	1–3 Interactions		
carbon (benzene)	carbon (carbonyl)	0.40	0.00
carbon (carbonyl)	carbon (carbonyl)	0.60	1.60

[a] 1–2 and 1–3 interactions refer to bond-stretching and angle-bending interactions, respectively.

parameters in order to obtain the best agreement with experimental geometries.

To this end, we have modified the EHMO program[30] by implementing (i) a quasi-Newton–Raphson gradient-based geometry optimizer[31] and (ii) a scanning procedure over a range of κ, δ values. Then for test compounds whose experimental structural properties are known, the relative root mean square (RRMS) of the error on calculated geometric parameters $P_i(calc)$ relative to the observed ones $P_i(exp)$ has been minimized:

$$RRMS = \left[\sum_{i=1}^{m} \left(\frac{[P_i(calc) - P_i(exp)]^2}{P_i(exp)^2} \right) \right]^{1/2} \quad (11)$$

where m is the number of independent parameters.

Our strategy in the search of optimum κ and δ values is the following: in order to be efficient and of a general use, the EHMO model builder is allowed to contain different sets of κ, δ parameters for the description of different atom–atom interactions and in particular metal–ligand interactions. In other words, a single set of κ, δ values should be able to lead to good predictions for a given type of metal–ligand interactions (i.e., carbonyls, aromatic rings, phosphine groups, etc.). In addition, we decided to limit ourselves to the first-row transition metal atoms and to use for all of them the same set of κ, δ parameters when coordinated to the same ligand. This procedure limits the number of κ, δ parameters to a minimum while being flexible enough to differentiate the various types of metal–ligand interactions encountered in organometallic chemistry; it is well known for instance that carbonyl ligands are better π acceptors than cyclopentadienyl rings and this should somehow be reflected by different choices of κ, δ parameters. However, in view of the deliberate strategy of using the same parameters for all the first-row transition metal atoms, the model could be more approximate when examining the variations of metal–ligand distances within series of compounds with the same ligands such as carbonyls or metallocenes.

It is clear, however, that the κ, δ parameters of K_{AB} (eq 10) corresponding to a long-range interaction which is not optimized should not be taken as variables. Together with the case of K values of both diagonal $H_{\mu\mu}$ and nondiagonal $H_{\mu\nu}$ elements on the same center, they are chosen as standard values: $\kappa = 0.75$, $\delta = 0.30$.

The values of the optimized κ, δ parameters are reported in Table I. In all the cases, we assumed that the internal geometry of the ligands (i.e., the C–O bond distance in metal carbonyls, the C–C and C–H bond lengths in metallocenes, etc.) may be kept frozen to standard values. Indeed, we have noticed that these structural parameters exhibit small variations within a given
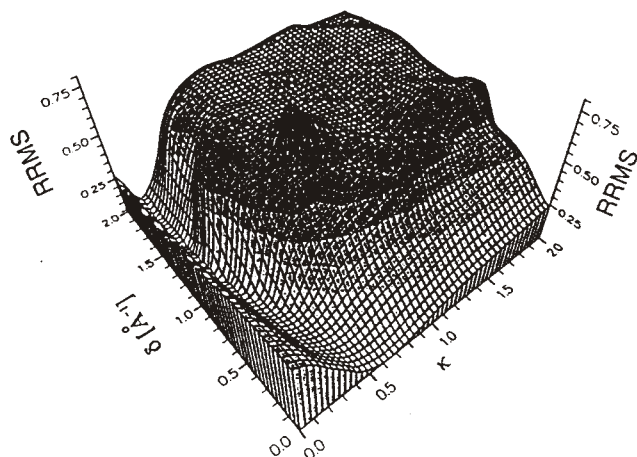
Figure 1. Three-dimensional map of RRMS values calculated as a function of κ and δ in the case of the optimization of Fe–C and C–O bond distances in $Fe(CO)_5$ assuming a D_{3h} structure and inequivalent axial and equatorial geometrical parameters. Experimental values are reported in Table II. The valley on the left corresponds to small RRMS values, i.e., to optimum κ, δ values.

series of organometallics and their optimization is much less important than that of the parameters involving the metal atom. The choice of κ, δ parameters for intraligand atom–atom interactions is therefore of little influence on the results and their values are reported in Table I. However, the values of these parameters may differ for interligand atom–atom nondiagonal EHMO matrix elements (see Table I) as they may reflect 1–3 interactions that are responsible for angle bending at the metal center.

III. Results and Discussion

Figure 1 presents a three-dimensional (3D) map corresponding to RRMS values calculated as a function of κ, δ parameters for $Fe(CO)_5$ while keeping the D_{3h} symmetry and optimizing separately the axial and equatorial distances. It is seen that a very narrow valley is obtained between the region corresponding roughly to $<\kappa, \delta> = <0.1, 2.0>$ to $<\kappa, \delta> = <0.5, 0.0>$. A detailed examination of the data corresponding to Figure 1 shows that the absolute minimum is found at $<\kappa, \delta> = <0.1, 1.9>$. We assume that this map can be considered as the one obtained if we had optimized the Fe–C distances (axial and equatorial) only as the C–O distances do not vary much. It is interesting to see that this valley extends along a region where κ, δ are approximately inversely proportional and this point will be treated below. A similar relation has been obtained for several complexes in which bond distances have been optimized.

A similar surface of RRMS values calculated as a function of κ, δ parameters is presented in Figure 2 in the case of (C_6H_6)-$Cr(CO)_3$ when optimizing the dihedral angle (Scheme I). A valley is again observed but, contrasting with Figure 1, it is very wide without exhibiting a particular absolute minimum. The relation between κ, δ along the valley is different from that found in Figure 1: increasing κ corresponds to increasing δ values along the bottom of the valley. The different behavior exhibited by the RRMS values in Figure 1 and 2 can be easily rationalized when looking at Figure 3, which displays K_{AB} as a function of R_{AB} for the H_2 molecule by using various δ values.

It is seen in Figure 3 that while K_{AB} is exponentially decreasing as a function of R_{AB} for any value of $\delta \neq 0$, all the curves cross at the point $<d_0, 1.75>$. Indeed, when $R_{AB} = d_0$, the exponential of eq 10 is equal to 1 and $K = 1 + \kappa$, i.e., 1.75. However the dependence of K_{AB} as a function of δ is different for $R_{AB} < d_0$ with respect to case for $R_{AB} > d_0$: in the first case increasing δ from 0 to 1 amounts to an increase in K_{AB} and therefore covalency; for $R_{AB} > d_0$, i.e., for A–B atoms exhibiting long-range
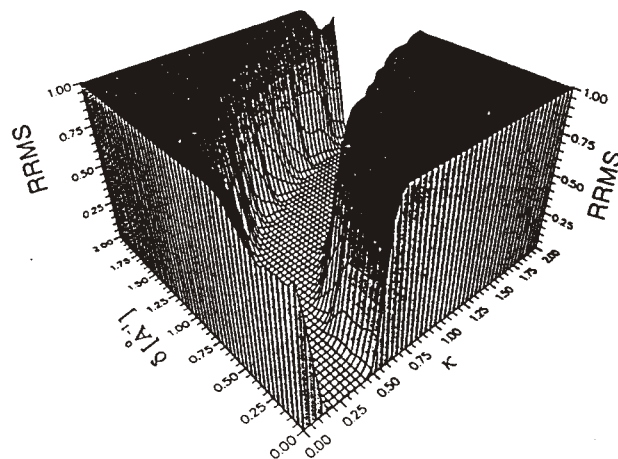

Figure 2. Three-dimensional map of RRMS values calculated as a function of κ and δ in the case of the optimization of the ring–metal–carbonyl dihedral angle (Scheme II) in $(\eta^6\text{-}C_6H_6)Cr(CO)_3$. The experimental value is reported in Table IV. The valley at the center corresponds to the optimum κ, δ values.
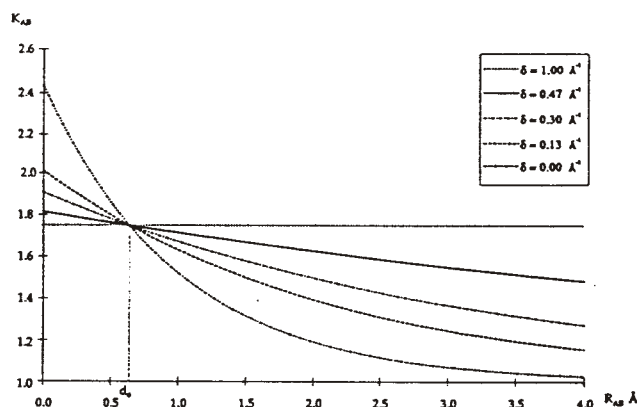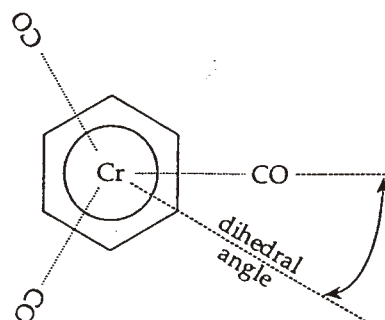

Figure 3. K_{AB} curves (eq 10) calculated as a function of R_{AB} for various values of the δ parameter in the case of the H_2 molecule with $\kappa = 0.75$ and $d_0 = 0.64$ Å.

SCHEME I

interactions, the opposite trend is observed and increasing δ amounts to a decrease in K_{AB} and therefore covalency. In the case of bonded atoms with $R_{AB} < d_0$, an increase of κ leads naturally to a decrease of δ as the model tends to compensate for an exaggerate increase in covalency. When $R_{AB} > d_0$, i.e., for nonbonded A–B atoms, any attempt to increase the covalent interaction between A–B atoms leads to a simultaneous increase of δ as in this case the model tries again to reduce an unreasonable increase of covalency. The fact that the interpretation of the behavior of optimum RRMS values as a function of κ, δ is rather easy is due to the simplicity of the EHMO approach and to the clear dependence of the results upon the parameters used.

The narrow valley displayed in Figure 1 suggests that for bonded atoms a relation may be found between κ, δ that would lead to a single parameter in eq 10. However this relation has been found to be typically dependent on the complex investigated and

TABLE II: Geometry Optimization of Metal Carbonyl Complexes with $\kappa = 0.10$ and $\delta = 1.90$ Å^{-1}

distance (Å)[a]	V(CO)$_6$[b]	Cr(CO)$_6$[c]	Fe(CO)$_5$[d]	Ni(CO)$_4$[e]
M–C$_{eq}$(calc)	1.909	1.856	1.834	1.305
M–C$_{eq}$(exp)	2.003	1.910	1.827	1.838
M–C$_{ax}$(calc)			1.806	
M–C$_{ax}$(exp)			1.806	
C–O$_{eq}$(calc)	1.160	1.146	1.150	1.154
C–O$_{eq}$(exp)	1.139	1.141	1.153	1.140
C–O$_{ax}$(calc)			1.140	
C–O$_{ax}$(exp)			1.153	
RRMS	0.053	0.024	0.011	0.017

[a] Eq corresponds to equatorial: ax corresponds to axial. This distinction applies only to Fe(CO)$_5$. [b] Reference 32. [c] Reference 33. [d] Reference 34. [e] Reference 35.

we have decided therefore to keep the two κ, δ parameters as independent variables, which leads in any case to more accurate predictions.

Table II summarizes the results of the geometry optimization of metal carbonyl complexes with a unique set of κ, δ values for the metal–carbonyl interaction. It is seen that the performance of the EHMO method in its improved form is reasonably good. For Fe(CO)$_5$ the model reproduces well the shortening of the axial metal–carbonyl distance with respect to the equatorial one. On the other hand we tried without success to optimize the κ, δ values for a carbon–carbon interaction in order to reproduce the 120° C–Fe–C equatorial angle of the bipyramidal complex. Apparently, this is due to the small value used for the κ parameter of the metal–carbonyl interaction. Indeed, when increasing this parameter, we have noticed that proper κ, δ values for C–C interaction can be found so as to lead to a 120° C–Fe–C equatorial angle. In this case, however, the Fe–C distance is significantly underestimated. Finally, it is seen in Table II that the metal–carbon distance is poorly predicted for V(CO)$_6$. This could be related to the fact that the ground state of the compound is known to exhibit a Jahn–Teller distortion.

The results obtained for the geometry optimization of metallocenes and dibenzene–metal complexes are reported in Table III. As mentioned in section II, the geometry optimizations have been performed in this case using a single set of κ, δ for all metallocenes and another one for dibenzene complexes. It is seen in Table III that again the predictions of the EHMO model compare reasonably well with experiment, the cases of ferrocene and vanadocene excepted. The qualitative trends in metal–ligand distance lengthening or shortening when going from vanadium to nickel are similar to those observed experimentally. The case of manganocene is interesting as this compound is known to exhibit a high-spin configuration in the ground state whereas its decamethyl analog is characterized by a low-spin configuration.[36] By using different populations for the predominantly metal 3d orbitals of manganocene so as to simulate a low-spin versus high-spin ground-state configuration, the modified EHMO model is able to reproduce adequately the lengthening of metal–ring distance accompanying the low-spin to high-spin transition. The lengthening is underestimated, however, probably because it is not possible to carry out spin-unrestricted calculations in the EHMO framework.

The results of the geometry optimization of organometallic complexes with mixed ligands are presented in Table IV. For

SCHEME II
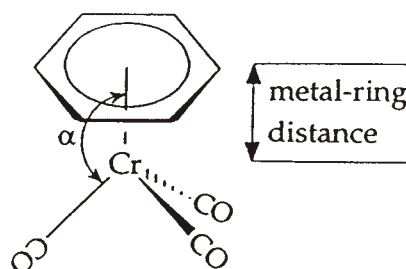
most of these compounds, the κ, δ parameters used for 1–2 interactions are those reported in Tables II and III, a few cases excepted (see footnotes of Table IV). In addition, the parameters for 1–3 interactions, i.e., C–ring–M–CO (Scheme I) and ring–M–CO (Scheme II) angles, have been optimized in the case of (C$_6$H$_6$)Cr(CO)$_3$. It is seen in Table IV that, as an average, the error bar on the M–ring distance (0.058 Å) is much larger than that on the M–CO distance (0.039 Å), which may be ascribed to (i) the significant number of compounds with substituted rings, for which the same κ, δ parameters as those of complexes with unsubstituted ligands have been used, and (ii) the variety of n-membered ligand rings encountered in the series of systems investigated. The M–L distances exhibit the largest deviation from experimental values, but it is of the same order as the M–ring distances. This can be explained by the fact that, in some cases, the same κ, δ parameters have been employed for different ligands. However, taken as a whole, the results presented in Table IV are rather satisfactory taking into account the approximations inherent to the semiempirical model used. In addition, no electron correlation nor multiplet structure description is explicitly introduced in the present calculations. A comparison is provided by the recent paper of Sosa et al.[59] which presents results obtained for the geometry optimization of organometallic complexes, generally carbonyls, using both local density functional (LDF) and SCF (3-21G basis set) methods. The average error bar exhibited by these results is 0.038 Å for LDF and 0.068 Å for SCF models, which is comparable to the errors reported in Table IV.

On the other hand, examination of Table IV reveals that both bond and dihedral angles are particularly well reproduced by the EHMO model: the average error is 2.6° for the former ones (with a large discrepancy of about 9° observed for (C$_5$H$_5$)Co-(CO)$_2$ and (C$_5$H$_5$)V(CO)$_4$) and the experimental dihedral angles are perfectly reproduced, although the energy difference between eclipsed and staggered conformations is generally of the order of 1 kcal/mol. Again the comparison with EHMO results obtained for organics shows that the present predictions are of alike accuracy.[22,23,28] Similarly, Sosa et al. report average error bars of 4.9° and 6.9° for bond angles calculated using the LDF and SCF models, respectively, which allows us to consider the performance of the EHMO predictions as satisfactory.

Finally, we present in Table V the results of a comparison between EHMO and both LDF and SCF results obtained for selected organometallic compounds. It is seen that again the EHMO model compares more favorably with experiment than the SCF one, while providing results of roughly the same accuracy as the LDF scheme. It has been shown recently, however, that the introduction of nonlocal corrections to the exchange and

TABLE III: Geometry Optimization of Metallocenes and Dibenzene–Metal Complexes[a]

	(C$_5$H$_5$)$_2$V[b]	(C$_5$H$_5$)$_2$Cr[b]	(C$_5$H$_5$)$_2$Mn[b]	(C$_5$H$_5$)$_2$Fe[b]	(C$_5$H$_5$)$_2$Co[b]	(C$_5$H$_5$)$_2$Ni[b]	(C$_6$H$_6$)$_2$V[c]	(C$_6$H$_6$)$_2$Cr[d]
distance (Å)								
M–ring(calc)	1.841	1.795	1.767/1.906[e]	1.745	1.756	1.781	1.682	1.630
M–ring(exp)	1.928	1.798	1.767/2.046[e]	1.661	1.739	1.828	1.660	1.613
RRMS	0.0451	0.0017	0.0000/0.0684	0.0506	0.0098	0.0257	0.0133	0.0105

[a] The values of κ, δ parameters are 0.5, 0.4 and 0.4, 0.5 for metallocenes and dibenzene–metal complexes, respectively. [b] Reference 36. [c] Reference 37. [d] Reference 38. [e] Metal–ring distance for low-spin/high-spin complexes.

TABLE IV: Geometry Optimization of Various Organometallic Complexes with Mixed Ligands

compounds	ref	distance (Å) M-ring calc	M-ring exp	M-CO calc	M-CO exp	M-L calc	M-L exp	angle (degrees) ring-M-CO calc	ring-M-CO exp	dihedral (degrees) C-ring-M-CO calc	C-ring-M-CO exp
$(C_5H_5)V(CO)_4$	39	1.889	1.930	1.880	1.900			109.6	118.0		
$(C_6H_4(NMe_2)_2)Cr(CO)_3$	40	1.646	1.732	1.820	1.784						
$(C_6H_5(NEt_2))Cr(CO)_3$	40	1.689	1.728	1.794	1.813						
$(C_6H_5Me)Cr(CO)_3$	40	1.683	1.725	1.814	1.824						
$(C_6H_5NH_2)Cr(CO)_3$	40	1.674	1.724	1.814	1.825						
$(C_6H_5OMe)Cr(CO)_3$	40	1.676	1.740	1.815	1.827						
$(C_6H_4(OMe)_2)Cr(CO)_3$	40	1.653	1.738	1.818	1.830						
$(C_6H_6)Cr(CO)_3$	41	1.656	1.730	1.836	1.842			124.4[a]	125.0[a]	30.0[a]	30.0[a]
$(C_6H_5(SiMe_3))Cr(CO)_3$	40	1.674	1.725	1.819	1.840						
$(C_6H_5COOMe)Cr(CO)_3$	40	1.685	1.719	1.814	1.842						
$(C_6H_5CHO)Cr(CO)_3$	40	1.684	1.717	1.814	1.845						
$(C_6H_5(C_2H_3))Cr(CO)_3$	42	1.739	1.709	1.830	1.838			123.5	125.0		
$(C_6H_4(COOMe)_2)Cr(CO)_3$	40	1.665	1.706	1.817	1.861						
$(C_{10}H_8)Cr(CO)_3$	43	1.812	1.745	1.834	1.821			126.1	125.0	30.0	30.0
$(C_{14}H_{10})Cr(CO)_3$[b]	44	1.807	1.756	1.834	1.824			126.1	125.0	30.0	30.0
$(C_{14}H_{10})Cr(CO)_3$[c]	45	1.799	1.731	1.835	1.843			126.3	125.8	30.0	30.0
$(C_5H_5)Mn(CO)_3$	46	1.738	1.798	1.935	1.800			126.0	123.8		
$(C_6H_6)Mn(CO)_3^+$	47	1.617	1.700	1.835	1.835			124.4	124.5	30.0	30.0
$(C_5H_5)Co(CO)_2$	48	1.767	1.813	1.778	1.679			128.7	119.1		
$(C_2H_4)Fe(CO)_4$	49			1.844/ 1.835[d]	1.836/ 1.800[d]	2.010[c,f]	1.990[c,f]				
$(C_2H_3CN)Fe(CO)_4$	50			1.840/ 1.848[d]	1.770/ 2.000[d]	1.947[c]	1.980[c]				
$(C_{10}H_8O)Fe(CO)_4$	51			1.871/ 1.878[d]	1.763/ 1.811[d]	1.875[c]	1.968[c]				
$(C_4H_6)Fe(CO)_3$	52	1.864	1.740	1.837	1.770			123.4	120.0		
$(C_4H_4)Fe(CO)_3$	53	1.661	1.725	1.799	1.819			124.0	121.3		
$(C_4H_4)(C_5H_5)Co$	54	1.718/ 1.793[g]	1.681/ 1.660[g]								
$(C_4H_4)_2Co^-$	54	1.704[h]	1.681[h]								
$(C_{10}H_8)_2Cr$	55	1.758[i]	1.764[i]								
$Cr(CO)_2(PH_3)_4$	56			1.874	1.817	2.310/ 2.319[j]	2.282/ 2.338[j]				
$Cr(CO)_3(PMe_3)_3$	57			1.867	1.838	2.479[k]	2.346[k]				
$Cr(CO)_5PMe_3$	57			1.864/ 1.868[d]	1.893/ 1.850[d]	2.281[k,l]	2.366[k,l]				
$(C_{14}H_{10})Cr(CO)_2PEt_3$[c]	58	1.826	1.731	1.872	1.817	2.323[k]	2.252[k]	127.1	126.7		
average difference		0.058		0.039		0.060		2.6		0.0	

[a] 1–3 interactions optimized for this compound (κ, δ for carbonyl–carbonyl and benzene–carbonyl interactions). [b] $C_{14}H_{10}$ corresponds to an anthracene ligand. [c] $C_{14}H_{10}$ corresponds to a phenanthrene ligand. [d] Corresponds to equatorial/axial metal–carbonyl distances, respectively. [e] Compound chosen to optimize κ, δ parameters for metal–ethylene 1–2 interaction. [f] Corresponds to metal–(C=C) distances. [g] Corresponds to metal–cyclobutadienyl/ metal–cyclopentadienyl distances, respectively. [h] Compound chosen to optimize κ, δ parameters for metal–cyclobutadienyl 1–2 interaction, the experimental geometry has been taken equal to the metal–cyclobutadienyl distance of the $(C_4H_4)Co(C_5H_5)$ complex, see ref 53. [i] Compound chosen to optimize κ, δ parameters for metal–naphthalene 1–2 interaction. [j] Corresponds to the cis/trans metal–phosphorus distances. [k] Corresponds to the metal–phosphorus distances. [l] Compound chosen to optimize κ, δ parameters for metal–phosphorus 1–2 interaction.

TABLE V: Comparison between Results Obtained with the Improved EHMO Model for Various Complexes and Those of More Elaborate Quantum Chemical Models

compound	exp	EHMO	LDF[a]	ab initio SCF[b]
$Cr(CO)_6$	1.910	1.856	1.874	1.922
$Fe(CO)_5$	1.827/1.807[c]	1.834/1.806[c]	1.778/ 1.776[c]	1.814/1.872[c]
$Ni(CO)_4$	1.838	1.805	1.794	1.838[d]
$(C_5H_5)_2V$	1.928	1.841		2.12
$(C_5H_5)_2Mn$	2.046[e]	1.906		1.95
$(C_5H_5)_2Fe$	1.661	1.745	1.60	1.89[d]/1.831[d]
$(C_5H_5)_2Co$	1.739	1.756		1.96
$(C_5H_5)_2Ni$	1.828	1.781		1.98
$(C_6H_6)_2Cr$	1.613	1.630		1.683
$(C_6H_6)Cr(CO)_3$	1.730/1.842[f]	1.656/1.836[f]		1.814/1.868[f]
$(C_5H_5)Mn(CO)_3$	1.798/1.800[f]	1.738/1.935[f]		1.917/1.883[f]

[a] References 6–7. [b] References 60–61. [c] Equatorial/axial Fe–CO distances. [d] Basis set optimized to obtain the best agreement with experiment. [e] High-spin compound. [f] Metal–ring/metal–CO distances.

correlation potential significantly improves the predictions of geometries carried out using the DF formalism.[61]

IV. Conclusions

The results reported above show that the EHMO method in its ASED form, when adequately parametrized, leads to geometry optimizations of organometallic compounds in satisfactory agreement with experiment. However, a major difficulty of this procedure lies in the fact that structural data of complexes with only one type of ligand are not always available. On the other hand, the comparison with more elaborate quantum chemical models is interesting: the error bars on the structural parameters obtained using the EHMO model are smaller than those found at the SCF level, whereas they are similar to those deduced from LDF calculations.

In addition, the simplicity of the method together with the minimal computational effort it involves suggest that the geometry of very large complexes with low symmetry could be reasonably predicted at relatively little expense in this model. In this case, however, such calculations should be performed only after adequate parametrization of κ, δ for 1–2, 1–3, and possibly 1–4 interactions. Further developments aiming at the parametrization of binuclear complexes and new types of ligands are in progress.

References and Notes

(1) Frühbeis, H.; Klein, R.; Wallmeier, H. *Angew. Chem., Int. Ed. Engl.* 1987, *26*, 403.

(2) Salahub, D. R. Ab initio Methods in Quantum Chemistry II. Adv. Chem. Phys. 1987, *64*, 447.

(3) Davidson, E. R. In *The Challenge of d and f Electrons. Theory and Computation*; Salahub, D. R., Zerner, M. C., Eds.; ACS Symp. Series 1989, *394*, 153.

(4) Bauschlicher, C. W.; Langhoff, S. R. *Int. Rev. Phys. Chem.* 1990, *9*, 149.

(5) Veillard, A. *Chem. Rev.* 1991, *91*, 743.

(6) Delley, B. *J. Chem. Phys.* 1991, *94*, 7245.

(7) Ziegler, T. *Chem. Rev.* 1991, *91*, 651.

(8) Salahub, D. R.; Fournier, R.; Mlynarski, P.; Papai, I.; St-Amant, A.; Ushio, J. In *Density Functional Methods in Chemistry*; Labanowski, J. K., Andzelm, J., Eds.; Springer: New York, 1991; p 77.

(9) Allinger, N. L.; Yuh, Y. H.; Lii, J. H. *J. Am. Chem. Soc.* 1989, *111*, 8551.

(10) Brubaker, G. R.; Johnson, D. W. *Coord. Chem. Rev.* 1984, *53*, 1.

(11) Boeyens, J. C. A. *Inorg. Chem.* 1985, *24*, 4149.

(12) Lauher, J. W. *J. Am. Chem. Soc.* 1986, *108*, 1521.

(13) Allured, V. S.; Kelly, C. M.; Landis, C. R. *J. Am. Chem. Soc.* 1991, *113*, 1.

(14) Atkinson, I. M.; Keene, R. F.; Gulbis, S. M.; Searle, G. H.; Tiekink, E. R. T. *J. Mol. Struct.* 1992, *265*, 189.

(15) Zerner, M. C.; Loew, G. H.; Kirchner, R. F.; Mueller-Westerhoff, U. T. *J. Am. Chem. Soc.* 1980, *102*, 589.

(16) Blyholder, G.; Head, J.; Ruette, F. *Theoret. Chim. Acta* 1982, *60*, 429.

(17) Li, J.; Jug, K. *J. Comput. Chem.* 1992, *13*, 93.

(18) Hoffmann, R. *J. Chem. Phys.* 1963, *39*, 1397.

(19) Anderson, A. B.; Hoffmann, R. *J. Chem. Phys.* 1974, *60*, 4271.

(20) Anderson, A. B.; *J. Chem. Phys.* 1975, *62*, 1187.

(21) Pensak, D. A.; McKinney, R. J. *Inorg. Chem.* 1979, *18*, 3407.

(22) Calzaferri, G.; Forss, L.; Kamber, I. *J. Phys. Chem.* 1989, *93*, 5366.

(23) Tupper, K. J.; Counts, R. W.; Gajewski, J. J. *Computers Chem.* 1991, *15*, 157.

(24) Weber, J.; Fluekiger, P.; Morgantini, P. Y.; Schaad, O.; Goursot, A.; Daul, C. *J. Comp. Aided Mol. Design* 1988, *2*, 235.

(25) Daul, C.; Goursot, A.; Morgantini, P. Y.; Weber, J. *Int. J. Quantum Chem.* 1990, *38*, 623.

(26) Weber, J.; Fluekiger, P.; Stussi, D.; Morgantini, P. Y. *J. Mol. Struct. (THEOCHEM)* 1991, *227*, 175.

(27) Weber, J.; Morgantini, P. Y.; Eisenstein, O. *J. Mol. Struct. (THEOCHEM)* 1992, *254*, 343.

(28) M. Brändle, G. Calzaferri, in preparation.

(29) Periodic table of the elements, Werner Meyer Ag, Hergiswil, Switzerland.

(30) (a) Howell, J.; Rossi, A.; Wallace, D.; Haraki, K.; Hoffmann, R. *QCPE Bull.* 1979, *11*, 344. (b) Calzaferri, G.; Brändle, M. *QCPE Bull.* 1992, *12*, in press. QCMP 116.

(31) Quasi-Newton gradient procedure, Davidon-Fletcher-Powell (DFP) routine, personal communication from Prof. C. Daul.

(32) Bellard, S.; Rubinson, K. A.; Sheldrick, G. M. *Acta Crystallogr.* 1979, *B35*, 271.

(33) Whitaker, A.; Jeffery, J. W. *Acta Crystallogr.* 1967, *23*, 977.

(34) Beagley, B.; Schmidling, G. *J. Mol. Struct.* 1974, *22*, 466.

(35) Hedberg, L.; Iijima, T.; Hedberg, K. *J. Chem. Phys.* 1979, *70*, 3224.

(36) Haaland, A. *Acc. Chem. Res.* 1979, *12*, 415.

(37) Radonovich, L. J.; Zuerner, E. C.; Efner, H. F.; Klabunde, K. J. *Inorg. Chem.* 1976, *15*, 2976.

(38) Haaland, A. *Acta Chem. Scand.* 1965, *19*, 41.

(39) Wilford, J. B.; Whitla, A.; Powell, H. M. *J. Organomet. Chem.* 1967, *8*, 495.

(40) Hunter, A.; Shilliday, L.; Furrey, W.; Zaworotko, M. *Organometallics* 1992, *11*, 1550.

(41) Rees, B.; Coppens, P. *Acta Crystallogr.* 1973, *B29*, 2515.

(42) Brown, G. M.; Frazier, C. C. *Acta Crystallogr.* 1989, *45*, 1158.

(43) Kunz, V.; Nowacki, W. *Helv. Chim. Acta* 1967, *50*, 1052.

(44) Hanic, F.; Mills, O. S. *J. Organomet. Chem.* 1968, *11*, 151.

(45) Muir, K. W.; Ferguson, G.; Sim, G. A. *J. Chem. Soc. (B)* 1968, 467.

(46) Berndt, A. F.; Marsh, R. E. *Acta Crystallogr.* 1963, *16*, 118.

(47) Gommans, L. H. P.; Main, L.; Nicholson, B. K. *J. Organomet. Chem.* 1985, *284*, 345.

(48) Beagley, B.; Parrot, C. T.; Ulbrecht, V.; Young, G. G. *J. Mol. Struct.* 1979, *52*, 47.

(49) Davis, M. I.; Speed, C. S. *J. Organomet. Chem.* 1973, *21*, 401.

(50) Luxmoore, P.; Truter, M. R. *Acta Crystallogr.* 1962, *15*, 1117.

(51) Raston, C. L.; Wege, D.; White, A. H. *Aust. J. Chem.* 1977, *30*, 2153.

(52) Mills, O. S.; Robinson, G. *Acta Crystallogr.* 1963, *16*, 758.

(53) Davis, M. I.; Speed, C. S. *J. Organomet. Chem.* 1970, *21*, 40.

(54) Riley, P. E.; Davis, R. E. *J. Organomet. Chem.* 1976, *113*, 157.

(55) Elschenbroich, Ch.; Möckel, R.; Massa, W.; Birkhahn, M.; Zenneck, U. *Chem. Ber.* 1982, *115*, 334.

(56) Huttner, G.; Schelle, S. *J. Cryst. Mol. Struct.* 1971, *1*, 69.

(57) Huttner, G.; Schelle, S. *J. Organomet. Chem.* 1973, *47*, 383.

(58) Kaftory, M. *Acta Crystallogr.* 1980, *36*, 2971.

(59) Sosa, C.; Andzelm, J.; Elkin, B. C.; Wimmer, E.; Dobbs, K. D.; Dixon, D. A. *J. Phys. Chem.* 1992, *96*, 6630.

(60) Almlöf, J.; Faegri, K.; Shilling, B. E. R.; Lüthi, H. P. *Chem. Phys. Lett.* 1984, *106*, 266.

(61) Williamson, R. L.; Hall, M. B. *Int. J. Quantum Chem., Quantum Chem. Symp.* 1987, *21*, 503.

(62) Fan, L.; Ziegler, T. *J. Chem. Phys.* 1991, *95*, 7401.